RESEARCH ARTICLE (Open Access)

3D Reconstruction of Bilayer and Honeycomb Scaffolds Used for the Treatment of Osteochondral Defects

TAULANT GOGA[1*], ERINDA LIKA[1], BLEDAR GOXHA[1]

[1]Faculty of Veterinary Medicine, Agricultural University of Tirana, 1025 Tirana, Albania;

*Corresponding author; E-mail: tgoga@ubt.edu.al

Abstract

Osteochondral defects represent a significant clinical challenge due to the limited regenerative capacity of articular cartilage and the complex interaction between cartilage and subchondral bone. The present study aimed to evaluate osteochondral regeneration using computed tomography (CT), based three-dimensional (3D) reconstruction and quantitative analysis of Hounsfield Unit (HU) values within regions of interest (ROI) following implantation of different biomaterial scaffolds in a sheep model. A total of 24 CT images of the knee joint in sheep were analyzed three months after surgical intervention. Four study groups were included: control (CNTR), Bilayer Wollastonite–Collagen (BWS), Honeycomb Hydroxyapatite–Wollastonite (HWS), and Honeycomb Hydroxyapatite–Magnesium–Collagen (HMG). Volumetric and densitometric parameters, including volume, minimum, maximum, mean and standard deviation (SD), were extracted from 3D ROI reconstructions. Statistical analysis was performed using non-parametric methods to identify significant differences between groups. The results demonstrated that the HMG (749.65 HU) and HWS (694,11 HU) groups exhibited higher HU values, indicating increased mineralization and improved tissue organization compared to the BWS (403.96 HU) and CNTR (326.02 HU) groups. The HMG group showed the highest mean HU values, suggesting superior osteogenic potential. Significant differences were observed mainly in the Max, SD, and Vol parameters, highlighting variations in tissue density and structural heterogeneity. In contrast, no significant differences were found for minimum and mean HU values across groups. CT-based 3D reconstruction and HU analysis provide a reliable, non-invasive approach for assessing osteochondral regeneration.

Keywords: Osteochondral defect; Scaffolds, Bilayer, Honeycomb.

1. Introduction

Tissue engineering represents one of the most dynamic fields of biomedical sciences, integrating principles of biology, medicine, and engineering to develop advanced solutions for restoring the function of damaged tissues. The main focus of this field is the combination of cells, biomaterials, and biological or physicochemical signals, with the aim of creating suitable conditions for the formation and organization of new functional tissues[1,2]. One of the key components in this process is the use of three-dimensional (3D) supporting matrics, known as "scaffolds," which provide a favorable environment for cell adhesion, proliferation, and differentiation. These structures not only offer mechanical support but can also be modified to actively interact with cells and guide regenerative processes[3]. Cells used in tissue engineering can be cells that are directly isolated and obtained from another site in the body and then placed directly into the area of interest[4], cells that form a three-dimensional tissue constructed or grown in vitro[5], or simply local cells near the defect site that participate in tissue regeneration in situ[6].

Scaffolds for tissue engineering are structures that mimic the properties of natural tissues and are highly porous to allow nutrient diffusion and cell migration[7]. In general, 3D scaffolds in tissue engineering function as an artificial extracellular matrix (ECM), and in some cases a temporary one, mimicking the structure and functionality of the natural ECM to physically guide or chemically instruct cellular responses and thereby promote tissue growth[8]. An ideal scaffold is composed of biocompatible and biodegradable materials in order to prevent unwanted immune reactions and to allow the complete replacement of the scaffold with regenerated tissue[9,10]. Scaffolds must also possess sufficient mechanical strength to be easily handled, withstand the physiological environment in which they will be

*Corresponding author: Taulant Goga; E-mail: tgoga@ubt.edu.al
(Accepted for publication 9.04.2026)
***ISSN**: 2218-2020, © Agricultural University of Tirana*

implanted, and influence cell growth, adhesion, and differentiation in a desirable manner.

The mechanical properties required for a 3D scaffold can vary significantly depending on the type of tissue and even the specific subregion of the tissue that is targeted for regeneration[11]. Composite scaffolds are an emerging strategy to overcome the limitations of single-layer scaffolds by combining different components to enhance overall performance. These materials integrate the most favorable properties of each constituent, leading to improved functionality. Composite scaffolds include one of the combinations; polymer–ceramic composites, which pair natural or synthetic polymers with ceramic layers, and polymer–polymer composites, which may involve natural, synthetic, or hybrid polymers[12,13]. Scaffolds are mostly used in the treatment of osteochondral defects and other pathologies related to the orthopedic field in both veterinary and human medicine, with challenging treatment due to the significant limitations of current techniques, particularly in terms of cartilage tissue regeneration[14,15]. Osteochondral defects involve damage to both the articular cartilage and the subchondral bone, presenting a complex clinical challenge because of the distinct biological and mechanical properties of these tissues. Articular cartilage is avascular and has a limited self-healing capacity, whereas subchondral bone is vascularized and can regenerate more easily. This imbalance complicates the development of effective osteochondral repair strategies[16]. An osteochondral lesion typically develops following a joint injury, such as repeated microtrauma or ischemia. The most affected individuals are those who participate in various athletic sports, as well as horses and large-breed dogs involved in physical activities, which are at higher risk of developing osteochondral lesions.These lesions may also be associated with genetic predisposition and abnormal bone development, particularly in young individuals.

Non-invasive imaging techniques play a crucial role in monitoring tissue regeneration processes, as they enable the assessment of structural and functional changes in tissues over time without the need for invasive procedures. Various imaging modalities, such as magnetic resonance imaging (MRI), computed tomography (CT), and micro-CT, are widely used in both preclinical and clinical studies to analyze bone defects.

Among these techniques, CT is considered one of the most important methods for evaluating bone regeneration, as it provides high-resolution three-dimensional images of bone structure and implanted biomaterials, allowing analysis of bone morphology, matrix integration, and the degree of mineralization of newly formed tissue[17]. CT uses X-rays to generate detailed cross-sectional images of the body and enables quantitative analysis of tissue density through Hounsfield Units (HU). HU values are based on the X-ray attenuation coefficient of tissues and are used to compare the density of biological materials. On this scale, water has a value of 0 HU, while air is around −1000 HU, whereas bone tissues exhibit much higher positive values, typically ranging from approximately 300 to 3000 HU, which are directly related to mineral content and bone density[18]. In bone regeneration studies, tissues with CT values between 700 and 2000 HU are considered newly formed bone, while values above this range may be associated with graft materials or residual non-biodegraded matrices within the region of interest[19].

The aim of this study was to perform a comprehensive evaluation of osteochondral regeneration through three-dimensional reconstruction and quantitative analysis of HU distribution within the region of interest (ROI) after treatment with different biomaterials of osteochondral defects. Specifically, the study was designed to assess the extent of tissue formation, mineralization, and integration of the implanted scaffolds three months after surgery in a sheep model. With the use of CT imaging and volumetric analysis, this approach enabled a detailed characterization of the spatial and densitometric properties of the regenerating tissue, providing insight into the effectiveness of the biomaterials in promoting osteochondral repair.

2. Material and Methods

2.1. Experimental design

In this study, a total of 24 tomographic images were included as part of the methodological analysis. These images were obtained from computed CT examinations of the knee joint performed three months after surgical intervention in sheep, used as a translational animal model. The inclusion of these images enabled a systematic evaluation of osteochondral regeneration and the effects of the implanted biomaterials under controlled experimental conditions. The sheep were randomly devided into four experimental groups. Two different scaffolds configurations were used, both consisting of a collagen component and a bioceramic component: a bilayer Wollastonite–Collagen configuration (BWS) and a “honeycomb” configuration in two variants, Hydroxyapatite–

Wollastonite (HWS) and Hydroxyapatite–Magnesium–Collagen (HMG). The term "honeycomb" was adopted because the structure of this configuration resembles, to some extent, the organization of a honeycomb.

- → Control group (CNTR): In this group were included 6 sheep and the osteochondral defect was created but left untreated to allow spontaneous healing.
- → Bilayer BWS: In this group were included 6 sheep and the osteochondral defects was treated with a bilayer BWS scaffold designed to mimic native osteochondral architecture through a dual-layer configuration supporting both cartilage and subchondral bone regeneration.
- → Honeycomb HWS group: In this group were included 6 sheep and the osteochondral defect was treated with a HWS composite scaffold.
- → Honeycomb HMG group: In this group were included 6 sheep and the osteochondral defect was treated with a HMG composite scaffold

2.2. Computed tomography analysis

Tomographic evaluations were performed in all individuals three months after the surgical intervention to assess osteochondral regeneration induced by the presence of the biomaterial. The right back limb was positioned in a craniocaudal orientation and scanned from the distal femoral diaphysis to the proximal tibial diaphysis using a 16-slice GE BrightSpeed CT scanner. The tomographic assessment protocol was conducted in spiral mode with the following acquisition parameters: slice thickness of 1.25 mm, 120 kVp, 200 mA, pitch 0.93, and a "bone plus" convolution kernel. A 3D reconstruction of the scanned area was subsequently generated. The 1.25 mm slice thickness was selected to ensure sufficient spatial resolution for the overall evaluation of subchondral bone mineral density and integration of the 3D scaffold, while maintaining acceptable radiation exposure and reasonable scanning time in a large animal model. This resolution is suitable for longitudinal in vivo monitoring of changes in mineralized tissues in clinically relevant osteochondral defects.

CT images were analyzed using the HOROS application. ROI were manually defined in four distinct areas of scaffold implantation within the osteochondral defect. ROI selection was performed using the Closed Polygon, CT-Bone, No CLUT, and Linear Table commands. Volumetric and densitometric parameters were extracted using the ROI Compute Volume function in the Horos DICOM Viewer, enabling a three-dimensional quantitative assessment of the osteochondral defect treated with the implanted 3D scaffolds (as it shown in Figure 1).

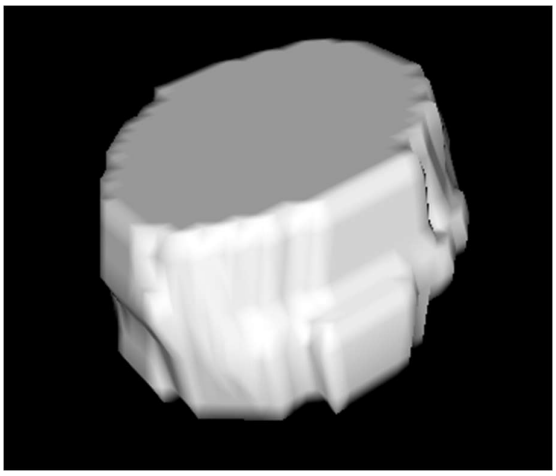

Figure 1 – Three-dimensional morphology reconstructed from ROI volume data.

Volume (cm^3) quantified the total size of the analyzed region, reflecting tissue formation within the defect area. The mean value (Mean, HU) represented the average radiological density and served as an indirect indicator of mineralized tissue deposition and bone regeneration. Minimum (Min) and maximum (Max) HU values described the density range within the ROI, allowing identification of areas with lower or higher values of mineralization. Standard deviation (SD) assessed the variability of HU values, providing information on the structural homogeneity of the regenerating tissue. Finally, the total (Tot) HU value represented the cumulative density of all parameters within the ROI, integrating volumetric and densitometric data to characterize the overall regenerative response to the implanted biomaterials.

2.3. Statistical analysis

All statistical analyses were performed using the Statistical Package for the Social Sciences (SPSS, version 17). Descriptive statistics were calculated for each variable, and the results are presented as mean ± SD. Prior to hypothesis testing, data distribution and homogeneity of variance were assessed. Since the data did not follow a normal distribution and the group sizes were relatively small, a non-parametric approach was considered appropriate. The Kruskal–Wallis test was used to evaluate overall differences between groups. This test is a rank-based non-parametric method used to determine whether two or more independent samples originate from the same distribution and is suitable for groups of unequal size or for variables that do not

follow a normal distribution[20]. Additionally, RStudio (version 2025.09.2+418) was used for graphical data presentation. To verify the robustness of the statistical results, the Kruskal–Wallis analyses were independently repeated in RStudio, yielding consistent results and confirming the statistical differences identified with SPSS.

3. Results and Discussion

All data included in this study were successfully analyzed about the HU values of the ROI Compute Volume parameters selected for this investigation. The ROI volume parameters obtained from the three-dimensional reconstruction of the implanted scaffolds illustrate how the values vary across the four study groups: CNTR, BWS, HMG and HWS. The mean values and standard deviations (SD) of the 3D ROI reconstructions for each study group are presented in Table 1.

The results indicate that the HMG and HWS biomaterials promote higher-quality osteochondral regeneration, characterized by greater density and a more organized structure, despite a lower volume compared to the control group. The HMG group exhibited the highest mean HU values (749.65 ± 103.32), followed by the HWS group (694.11 ± 107.48), whereas the BWS (403.96 ± 88.17) and CNTR (326.02 ± 110.42) groups showed lower values. This suggests a higher density of mineralized tissue in the HMG and HWS groups. The significantly higher mean HU values observed in the HMG and HWS groups suggest enhanced mineral deposition and more advanced bone formation. HU values are widely recognized as an indirect indicator of bone mineral density and tissue maturation, with higher values corresponding to increased mineral content and mechanical competence of the regenerated tissue[18,19]. Maximum HU values were also higher in the HMG and HWS groups, reflecting a more advanced degree of mineralization. In contrast, the CNTR group presented lower values, confirming the lack of effective regeneration. Volume parameters did not show marked differences among the groups, while the higher SD observed in the experimental groups suggests greater heterogeneity in the regenerated tissue. In this context, the HMG group, which exhibited the highest HU values, appears to support a more effective osteogenic response, potentially due to the synergistic effects of hydroxyapatite, magnesium, and collagen. Magnesium biomaterials have been reported to enhance osteoblast activity and promote bone regeneration through improved cellular signaling and biodegradation profiles[21]. Similarly, in the present study, the three-dimensional reconstruction assessment demonstrated consistent results with the our previously reported ROI value analysis, indicating that the HMG scaffold exhibits superior outcomes compared to the other groups[17].

Table 1 – HU values of ROI volumetric parameters across the study groups (CNTR, BWS, HWS, and HMG).

Group	ROI Compute Volume values					
	Volume (cm^3)	*Min (HU)*	*Max (HU)*	*Mean (HU)*	*SD (HU)*	*Total (HU)*
CNTR	*0,91 ± 0,2*	*-104,83 ± 104,7*	*1506 ± 293,25*	*326,02 ± 110,42*	*312,71 ± 61,17*	*2782168,17 ± 1116407,8*
BWS	*0,65 ± 0,2*	*-76,67 ± 176,65*	*1586,33 ± 767,46*	*403,96 ± 88,17*	*286,78 ± 102,71*	*2049831,83 ± 1179683,8*
HMG	*0,51 ± 0,16*	*-122,83 ± 193,04*	*2944,83 ± 195,55*	*749,65 ± 103,32*	*518,01 ± 120,18*	*2871595,33 ± 663089,53*
HWS	*0,61 ± 0,1*	*-100,17 ± 185,39*	*2850,5 ± 291,32*	*694,11 ± 107,48*	*460,16 ± 106,65*	*3115297,83 ± 1218194,3*

The statistical analysis was performed for the ROI volume parameters to identify significant differences between the study groups. Statistical significance was indicated with * for $p < 0.05$ and ** for $p < 0.01$, as illustrated in Figure 2. The heatmap presents the p-values for comparisons among the study groups (CNTR, BWS, HMG, and HWS) for the ROI Compute Volume parameters. Statistically significant

differences ($p < 0.05$ and $p < 0.01$) were mainly observed for the Max, SD, and Vol parameters, with the HMG group showing pronounced differences compared to the CNTR and BWS groups.

The Max parameter exhibited significant variations in most intergroup comparisons, suggesting considerable differences in the maximum tissue density. The SD parameter also showed significant differences, reflecting variations in the structural homogeneity of the regenerated tissue, particularly between the HMG group and the other groups. For the Vol parameter, significant differences were mainly observed in comparisons involving the CNTR and BWS groups.

In contrast, the Min and Mean parameters did not show statistically significant differences between the groups, suggesting lower variability in the minimum and average tissue density across the study groups.

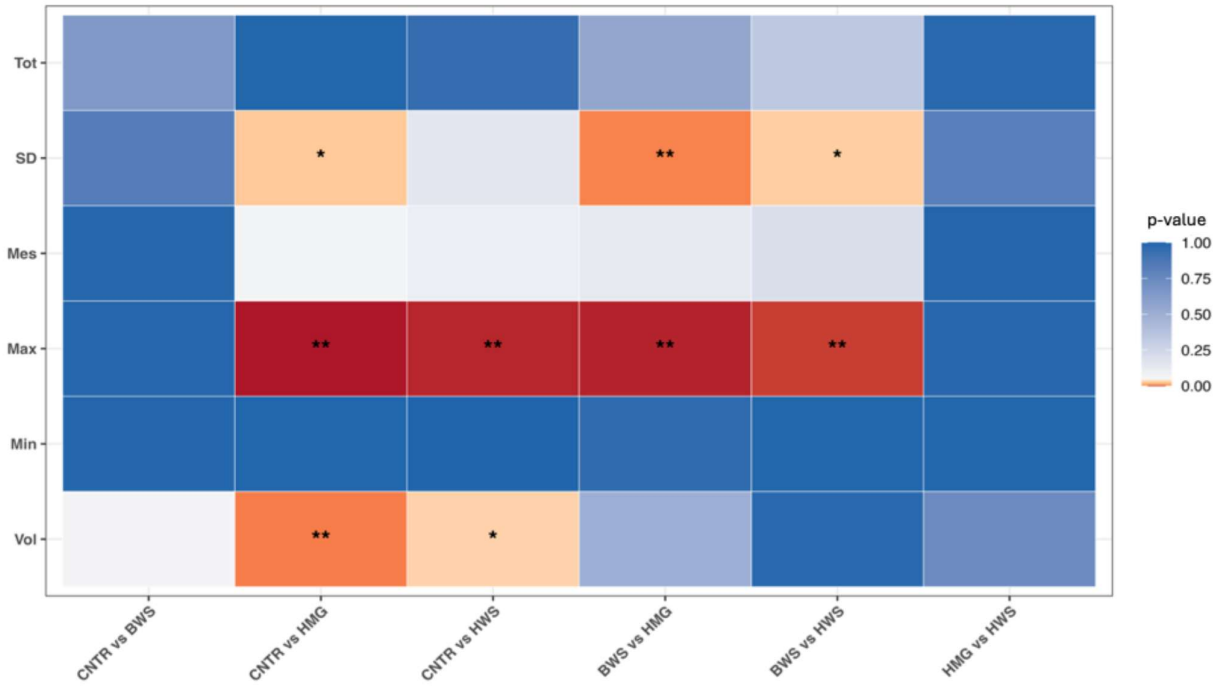

Figure 2 – Heatmap of the statistical comparisons of ROI volumetric parameters among the study groups, where * indicates $p < 0.05$ and ** indicates $p < 0.01$.

Overall, these results support the hypothesis that composite biomaterials combining collagen with bioactive ceramics, particularly those incorporating hydroxyapatite and magnesium, enhance osteochondral regeneration by promoting both mineralization and structural integration. The use of CT-derived HU analysis and 3D reconstruction proves to be a valuable, non-invasive tool for longitudinal assessment of biomaterial performance in translational large-animal models.

However, some limitations should be acknowledged. The relatively small sample size and the single time point (3 months) may not fully capture the long-term remodeling and maturation of the regenerated tissue. Future studies incorporating longer follow-up periods, histological correlation, and biomechanical testing would provide a more comprehensive understanding of scaffold performance.

4. Conclusions

In conclusion, the present study demonstrates that CT-based three-dimensional reconstruction and HU analysis are effective tools for evaluating osteochondral regeneration. Among the tested biomaterials, the HMG scaffold showed the most promising results, characterized by higher tissue density and improved structural organization compared to the other groups. These findings highlight the potential of composite biomaterials, particularly those incorporating hydroxyapatite and magnesium, to enhance osteochondral repair and support their application in translational regenerative strategies.

6. References

1. Kim YS, Smoak MM, Melchiorri AJ, et al. An Overview of the Tissue Engineering Market in the United States from 2011 to 2018. *Tissue Engineering Part A* 2019; 25: 1–8.
2. Langer R, Vacanti JP. Tissue Engineering. *Science* 1993; 260: 920–926.
3. Chan BP, Leong KW. Scaffolding in tissue engineering: general approaches and tissue-specific considerations. *Eur Spine J* 2008; 17: 467–479.
4. Gao C, Seuntjens J, Kaufman GN, et al. Mesenchymal stem cell transplantation to promote bone healing. *Journal of Orthopaedic Research* 2012; 30: 1183–1189.
5. Daly AC, Sathy BN, Kelly DJ. Engineering large cartilage tissues using dynamic bioreactor culture at defined oxygen conditions. *J Tissue Eng* 2018; 9: 2041731417753718.
6. Liu M, Nakasaki M, Shih Y-RV, et al. Effect of age on biomaterial-mediated in situ bone tissue regeneration. *Acta Biomater* 2018; 78: 329–340.
7. Yang S, Leong KF, Du Z, et al. The design of scaffolds for use in tissue engineering. Part I. Traditional factors. *Tissue Eng* 2001; 7: 679–689.
8. Howard D, Buttery LD, Shakesheff KM, et al. Tissue engineering: strategies, stem cells and scaffolds. *Journal of Anatomy* 2008; 213: 66–72.
9. Haugh MG, Murphy CM, McKiernan RC, et al. Crosslinking and mechanical properties significantly influence cell attachment, proliferation, and migration within collagen glycosaminoglycan scaffolds. *Tissue Eng Part A* 2011; 17: 1201–1208.
10. Murphy CM, O'Brien FJ, Little DG, et al. Cell-scaffold interactions in the bone tissue engineering triad. *Eur Cell Mater* 2013; 26: 120–132.
11. Morgan EF, Unnikrisnan GU, Hussein AI. Bone Mechanical Properties in Healthy and Diseased States. *Annu Rev Biomed Eng* 2018; 20: 119–143.
12. Khan AR, Gholap AD, Grewal NS, et al. Advances in smart hybrid scaffolds: A strategic approach for regenerative clinical applications. *Engineered Regeneration* 2025; 6: 85–110.
13. Lu Y, Wang X, Chen H, et al. "Metal-bone" scaffold for accelerated peri-implant endosseous healing. *Front Bioeng Biotechnol* 2024; 11: 1334072.
14. Bader DL, Salter DM, Chowdhury TT. Biomechanical Influence of Cartilage Homeostasis in Health and Disease. *Arthritis* 2011; 2011: 1–16.
15. Crovace AM, Giancamillo AD, Gervaso F, et al. Evaluation of in Vivo Response of Three Biphasic Scaffolds for Osteochondral Tissue Regeneration in a Sheep Model. *Veterinary Sciences* 2019; 6: 90.
16. Constance Lesage, Marianne Lafont, P. Guihard, et al. Material-Assisted Strategies for Osteochondral Defect Repair. *Advanced Science*; 9. Epub ahead of print 24 March 2022. DOI: 10.1002/advs.202200050.
17. Goga T, Goxha B, Crovace AM, et al. Tomographic Assessment of Bone Regeneration in Osteochondral Lesion Treated with Various Biomaterials in a Sheep Model Study. *JFB* 2025; 16: 120.
18. Simion G, Eckardt N, Senft C, et al. Bone density of the axis (C2) measured using Hounsfield units of computed tomography. *J Orthop Surg Res* 2023; 18: 93.
19. Buenger F, Sakr Y, Eckardt N, et al. Correlation of quantitative computed tomography derived bone density values with Hounsfield units of a contrast medium computed tomography in 98 thoraco-lumbar vertebral bodies. *Arch Orthop Trauma Surg* 2022; 142: 3335–3340.
20. Kruskal WH, Wallis WA. Use of Ranks in One-Criterion Variance Analysis. *Journal of the American Statistical Association* 1952; 47: 583–621.
21. Zhenkang W, Lei L, ZHANG H, et al. Magnesium-Containing Implants Enhance Bone Healing: A Mechanobiological Perspective. *Mechanobiology in Medicine* 2025; 3: 100161.